



Effect of austenitic texture on tensile behavior of lean duplex stainless steel with transformation induced plasticity (TRIP)

Jun-Yun Kang^{a,*}, Hoyoung Kim^a, Kyung-Il Kim^b, Chang-Hoon Lee^a, Heung Nam Han^b,
Kyu-Hwan Oh^b, Tae-Ho Lee^a

^a Korea Institute of Materials Science, 797 Changwon-daero, Seongsan-gu, Changwon, Gyeongnam 51508, Republic of Korea

^b Department of Materials Science and Engineering and Research Institute of Advanced Materials, Seoul National University, 1 Gwanak-ro, Gwanak-gu, Seoul 08826, Republic of Korea

ARTICLE INFO

Keywords:

Steel
Austenite
Mechanical characterization
Martensitic transformation
Texture

ABSTRACT

Mechanically induced martensitic transformation (MIMT) and consequent plastic flow behavior with respect to austenitic texture were investigated in a lean duplex stainless steel. Different grain sizes and textures with fixed phase fractions were obtained via varying the thermomechanical processes. Nearly random distribution of austenitic orientation exhibited a distinguished flow curve from the others with a major $D\{4\ 4\ 11\}\langle 11\ 11\ 8\rangle$ component due to more gradual enhancement of hardening by less martensitic transformation. In order to compare the susceptibility to the transformation with respect to individual austenitic orientations and the experimental textures, interaction energy between the imposed stress and transformation strain was calculated by a classical transformation and a crystal plasticity model. The results indicated that a larger stress imposed on the D component led to higher interaction energy and a steeper progress of MIMT observed in the textured materials.

1. Introduction

Duplex stainless steels (DSS) have microstructures that consist of similar fractions of face centered cubic (fcc) austenite and body centered cubic (bcc) ferrite [1]. By virtue of constructive property combinations between the two constituent phases, they usually show an excellent balance in mechanical properties as well as corrosion resistance. They are used in many applications in chemical, petroleum, and atomic energy industries [2–5], and have progressively substituted for some classical austenitic stainless steels since the 1990s [6].

Lean DSSs have been developed to reduce the initial material cost in production and cost instability by reduction of expensive alloy elements [6–11]. As a major strategy to design lean compositions, inexpensive austenite stabilizers such as N and Mn have been added to lower the content of an expensive one, i.e., Ni [6–11]. In addition to the effect of austenite stabilization, Mn increases the solubility of the interstitial element N [12,13] which gives potent solid solution strengthening [13,14] and improves the resistance to pitting corrosion [13,15]. Therefore, in spite of the leaner compositions, some lean alloys reported superior mechanical properties and corrosion resistance [9–11].

Recently, a few lean DSSs with exceptionally good tensile properties

by transformation induced plasticity (TRIP) were introduced [16–21]. In these alloys, the mechanically induced martensitic transformation (MIMT) in metastable austenite enhanced their strain hardening capacity, and the extended progress of MIMT to a large strain resulted in a very high tensile strength and ductility over 1 GPa and 60% respectively [18]. From the consideration on N content and its partitioning between the phases, stacking fault energy (SFE) which determined the deformation mechanisms of austenite was estimated to be in the range for MIMT [19,20]. Detailed microscopic analyses were performed to interpret the relationship between the progress of MIMT and tensile behavior, which confirmed the beneficial effect of MIMT on the excellent plasticity [20,21]. A number of studies followed to reveal the effect of various factors on this TRIP effect [21–24]. It is known that the strength and the ductility increased with an increasing content of N because of the increasing volume of mechanically induced martensite [21]. It was also reported that enhanced MIMT below room temperature increased uniform elongation [22], while an increased strain rate [23] and annealing temperature [24] suppressed MIMT. However, in spite of these studies, less focus was put on the probable effect of grain size, orientation or texture. In this article, the effect of austenitic texture on characteristic tensile behavior by TRIP is analyzed and discussed using a TRIP-aided lean DSS, which additionally

* Corresponding author.

E-mail address: frice@kims.re.kr (J.-Y. Kang).

Table 1
Chemical composition of the lean duplex stainless steel (wt%).

Cr	Mn	Mo	W	C	N	Si
18.28	5.68	2.38	0.39	0.035	0.300	0.11

contributes to the development of lean DSSs with tailored properties.

2. Experimental

The composition of the alloy is presented in Table 1. An ingot of 9 kg weight was cast using vacuum induction melting. It was reheated to 1200 °C, held for 2 h, hot rolled between 1100 and 950 °C and quenched in water. The thickness reduction in the hot rolling was 82.5% (from 40 mm to 7 mm). A part of the hot band was annealed at 1050 °C for 30 min, quenched in water, and denoted as HR30. The remaining parts were cold rolled by a thickness reduction of 82% (from 7 to 1.25 mm), also annealed at 1050 °C for 5 or 120 min and quenched. The former was denoted as CR5 and the latter as CR120. The designations of the above specimens simply represent the process prior to the annealing, i.e., hot rolling (HR) or cold rolling (CR), and the durations of the final annealing at 1050 °C, i.e., 5, 30 or 120 min.

Uniaxial tensile tests of the specimens were conducted at room temperature using a universal test machine (Instron 5882) with a crosshead speed of 2 mm/min, i.e., an initial strain rate of $1.33 \times 10^{-3} \text{ s}^{-1}$. The preparation of the specimens and the test procedure followed the instructions in ASTM E8 [25]. The microstructures of the specimens were characterized using an electron backscatter diffraction (EBSD) system, Oxford Instruments NordlysNano detector with AZTEC software in a field emission scanning electron microscope (FESEM), JEOL JSM-7001F. EBSD mappings in the mid-thickness regions of the specimens were conducted on electropolished surfaces that were normal to the transverse direction (TD). This microtexture analysis presented the morphological characteristics of grains, fractions and textures of the two constituent phases, ferrite (α) and austenite (γ). The electropolishing was carried out using a commercial electropolisher (Struers LectroPol5) with a solution of 90 vol% ethanol and 10 vol% perchloric acid at -20 °C. For statistical reliability in the analyses, the total mapping area per specimen covered 0.8–3.2 mm² depending on the grain size (at least 10,000 grains per phase).

3. Results

The microstructures of the specimens are presented in Fig. 1 via the overlay images of phase, boundary and band contrast maps constructed from the EBSD mappings. The clustering of each phase and the consequent banded structures were observed. The average grain sizes and phase fractions are listed in Table 2. All the specimens were constituted by nearly the same phase fractions due to the same annealing temperature. It was clear that the minimum duration of annealing, i.e., 5 min for CR5, was sufficient to attain the fully annealed and equilibrated microstructure because of the applied high tempera-

Table 2
Average phase fractions and grain sizes in equivalent circle diameter (ECD).

Phase		CR5	CR120	HR30
α	Fraction (%)	41.1	42.4	42.5
	Grain size (μm)	2.72	9.82	9.10
γ	Fraction (%)	58.9	57.6	57.5
	Grain size (μm)	3.31	10.27	13.54

ture (1050 °C). Considerable grain growth occurred in the prolonged annealing of CR120 in which the average grain diameter increased to more than three times from that of CR5. At a brief glance, HR30 exhibited the largest grain size in Fig. 1 because of some coarse grains. However, its average grain sizes were comparable to those of CR120 in Table 2. The broader grain size distribution in HR30 could be attributed to the omission of cold rolling, while the ratio of its maximum grain size to that of CR120 was less than 3 (80 μm in HR30 vs. 30 μm in CR120) which was less than the average grain size ratio of CR120 to CR5.

Fig. 2(a) presents the tensile flow curves, and the average tensile properties are listed in Table 3. As expected from the grain size distributions in Fig. 1 and Table 2, CR5 had the highest stress evolution, followed by CR120. All the specimens exhibited very high tensile strength of over 800 MPa with large elongations exceeding 60%. Characteristic upward deflections of the flow curves were observed, which were more definite for CR5 and CR120 (indicated by the broken circle). The less definite deflection of HR30 led to a distinct shape of the curve, and the dissimilarity increased with strain (indicated by a double-sided arrow). Fig. 2(b) corresponds to the strain hardening rate obtained from Fig. 2(a). All the specimens experienced a transient increase in the hardening rate after their respective local minimum values, σ_b (marked with arrows). Fig. 2(c) is the normalization of Fig. 2(b) with the respective σ_b . It shows more clearly that HR30 exhibited later, slower and more gradual enhancement in hardening. This distinctive hardening behavior would explain the distinct shape of the flow curve as well as the increasing dissimilarity with strain.

Figs. 3 and 4 present the orientation distribution function (ODF) of austenite and ferrite, respectively, in the $\phi_2=45^\circ$ section of the Euler space (notation by Bunge [26]), in which most of major texture components could be shown. For convenience, the major components found in this study are listed in Table 4. CR5 and CR120 had almost identical austenitic textures of moderate intensity as shown in Fig. 3. They were made up primarily of the D component with a very weak Goss component. As shown in Fig. 3(c), the peak ODF value for HR30 was too small, thus, the austenitic orientation distribution could be regarded as random. In Fig. 4, RC (rotated cube) was the common primary component of ferritic textures for all the specimens. CR5 and CR120 show the typical types of textures observed in many cold rolled and annealed ferritic steels [27,28]. While the ferritic texture of CR5 more resembled cold rolling textures which were represented as a strong partial RD// $\langle 110 \rangle$ fiber component, that of CR120 was closer to annealing textures with weakened RD// $\langle 110 \rangle$ and enhanced ND//

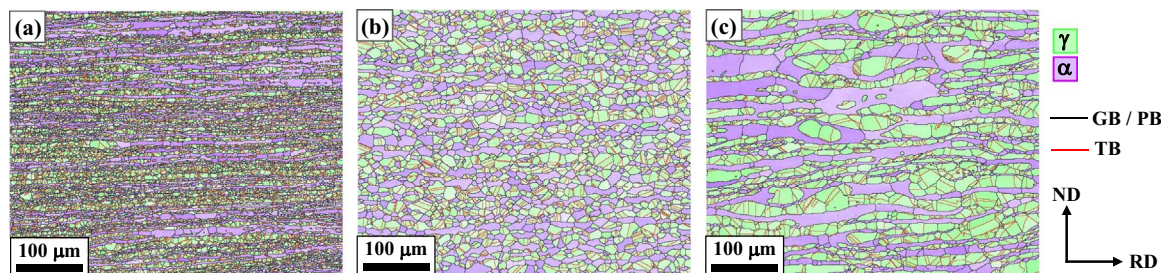


Fig. 1. Microstructures according to the process conditions (overlay of phase, band contrast and boundary maps from EBSD): (a) CR5, (b) CR120, (c) HR30 (γ : austenite, α : ferrite, GB: grain boundary whose disorientation exceeds 3°, PB: phase boundary, TB: twin boundary, ND: normal direction, RD: rolling direction).

Download English Version:

<https://daneshyari.com/en/article/5456474>

Download Persian Version:

<https://daneshyari.com/article/5456474>

[Daneshyari.com](https://daneshyari.com)